TECHNICAL PAPER

ISSN 1047-3289 *J. Air & Waste Manage. Assoc.* **55**:1019–1030

Integrated Assessment Modeling of Atmospheric Pollutants in the Southern Appalachian Mountains. Part I: Hourly and Seasonal Ozone

James W. Boylan, Mehmet T. Odman, James G. Wilkinson, and Armistead G. Russell
School of Civil and Environmental Engineering, Georgia Institute of Technology, Atlanta, GA

Kevin G. Doty, William B. Norris, and Richard T. McNider
University of Alabama in Huntsville, Huntsville, AL

ABSTRACT

Recently, a comprehensive air quality modeling system was developed as part of the Southern Appalachians Mountains Initiative (SAMI) with the ability to simulate meteorology, emissions, ozone, size- and composition-resolved particulate matter, and pollutant deposition fluxes. As part of SAMI, the RAMS/EMS-95/URM-1ATM modeling system was used to evaluate potential emission control strategies to reduce atmospheric pollutant levels at Class I areas located in the Southern Appalachians Mountains. This article discusses the details of the ozone model performance and the methodology that was used to scale discrete episodic pollutant levels to seasonal and annual averages. The daily mean normalized bias and error for 1-hr and 8-hr ozone were within U.S. Environment Protection Agency guidance criteria for urban-scale modeling. The model typically showed a systematic overestimation for low ozone levels and an underestimation for high levels. Because SAMI was primarily interested in simulating the growing season ozone levels in Class I areas, daily and seasonal cumulative ozone exposure, as characterized by the W126 index, were also evaluated. The daily ozone W126 performance was not as good as the hourly ozone performance; however, the seasonal ozone W126 scaled up from daily values was within 17% of the observations at two typical Class I areas of the SAMI region. The overall ozone performance of the model was deemed acceptable for the purposes of SAMI's assessment.

IMPLICATIONS

Three-dimensional, grid-based photochemical models can be used to quantify source-receptor relationships and assess emission control strategies to help improve air quality. In the past, independent models were used to simulate ozone, particulate matter, and deposition (wet and dry) separately. Here, a comprehensive modeling system for multiple atmospheric pollutants is used to conduct an integrated assessment of emission impacts and controls on the Southern Appalachian Mountains. Traditionally, ozone modeling has focused on peak 1-hr concentrations in the urban areas to show attainment with the National Ambient Air Quality Standards. This project differs by focusing on rural monitoring sites and evaluating a cumulative ozone exposure index (W126) that will be used to quantify impacts on forests and crops.

INTRODUCTION

Adverse air pollution effects on visibility, streams, soil, and vegetation have been documented in the national parks, forests, and wilderness areas of the Southern Appalachian Mountains in the eastern United States.[1,2,3] These impacts were studied by the Southern Appalachian Mountains Initiative (SAMI). SAMI was a nonprofit entity made up of participants from various stakeholder groups including state and federal government agencies, industry, academia, and special interest groups. The goal of SAMI was to assess the air quality, health, and ecosystem benefits of emission control strategies that could be used to mitigate air quality-related impacts from ozone, particulate matter (PM), and acid deposition.

A comprehensive atmospheric modeling system was developed to help SAMI achieve its goals by simulating the complex chemical and physical processes that govern the formation and removal of gas and aerosol-phase pollutants in the atmosphere. This atmospheric modeling system consists of the Urban-to-Regional Multiscale–One Atmosphere Model (URM-1ATM),[4] the Regional Atmospheric Modeling System (RAMS),[5] and the Emission Modeling System (EMS-95).[6] The URM-1ATM air quality model is based on the URM model[7,8] and has been enhanced to include aerosol dynamics, heterogeneous sulfate formation, and wet deposition scavenging processes. To use this modeling system with confidence, model predictions are evaluated against observations. Prior performance of the

URM model had been conducted for ozone only.[8,9] With the enhanced version of the model, a more extensive evaluation of the URM-1ATM model has been conducted here.

SAMI adopted an episodic modeling approach to quantitatively assess the atmospheric response to different emission strategies under a variety of conditions for use in an integrated assessment considering seasonal ozone, annual visibility, and annual deposition impacts. Part of this approach was to develop a method for characterizing discrete time intervals by a statistically-defined category or class depending on type of air quality impact and meteorology.[12] These classes, which varied by site and type of impact, were then used to select a set of multi-day episodes to represent the full spectrum of ozone, visibility, and deposition that occurred between the years 1991 and 1995. Whereas it is true that other studies have performed ozone simulations for full summer seasons,[10,11] SAMI's decision to use a "one-atmosphere" approach to model ozone, PM, and acid deposition simultaneously made it computationally impractical to model all days in a period of several years and assess the effectiveness of a large number of control strategies. The errors associated with using this episodic approach to represent entire seasons or years are small compared with the uncertainties associated with the modeling system. In this article, ozone model performance for four of the six multiday episodes (consisting of 46 discrete episode days) is evaluated in detail.

Model Description

The URM-1ATM is a comprehensive, three-dimensional Eulerian, multi-phase photochemical air quality model that accounts for the emissions, transport, chemical transformation, and wet and dry deposition of pollutants in the atmosphere. The model uses a finite element, variable mesh transport scheme.[7] The gas-phase reaction kinetics are described using the SAPRC chemical mechanism.[13,14] Aerosol dynamics are simulated using ISORROPIA[15] for inorganic thermodynamic equilibrium, organic aerosol yields from volatile organic compound oxidation,[16] and the moving sectional approach[17] for particle growth/shrinkage. The Reactive Scavenging Module[18] is used for wet deposition scavenging processes and a three-resistance approach based on the formulation of Wesely[19] is used for dry deposition. More detailed information about URM-1ATM can be found in Boylan et al.[4]

A modified version of the Regional Atmospheric Modeling System (RAMS)[5] version 3a is used to produce meteorological input fields for the air quality model. The RAMS was configured for a grid structure of three nested grids and run in nonhydrostatic mode with cloud and rainwater microphysics activated. The main data source for meteorological simulations was the National Centers for Environmental Prediction/National Center for Atmospheric Research reanalysis data.[20] Specific details of the meteorological modeling can be found in Doty et al.[21]

Day-specific, hourly, speciated emissions were developed for each episode using the Emission Modeling System.[6] Point source, area source, and on-road mobile source emission estimates produced by the EMS-95 were based on a 1990 inventory developed by the Pechan/Avanti Group[22] for SAMI. The on-road mobile source data (e.g., vehicle miles traveled by state, county, and roadway type; vehicle mix by state, county, and roadway type; speeds by vehicle type and roadway type) were used to estimate on-road mobile source emissions by the EMS-95 Motor Vehicle Emissions Model.[6] This model uses MOBILE5b[23] to compute vehicle-dependent emissions factors of carbon monoxide (CO), nitrogen oxides (NO_X), and total organic gases. Biogenic emissions were estimated using the U.S. Environmental Protection Agency's (EPA's) Biogenic Emissions Inventory System, version 2.[24,25] Point source emissions estimates were enriched with day-specific emissions data obtained from major utility companies in the modeling region. Meteorological model results were used to estimate the temperature and radiation dependent biogenic emissions and the temperature-dependent on-road mobile source emissions. A comprehensive list of emitted species can be found in Boylan et al.[4]

Modeling Domain and Grid

Figure 1a shows the nested horizontal grid structure used by RAMS for the July 1995 episode. The coarse, intermediate, and fine grids had resolutions of 48-, 24-, and 12-km, respectively. Simulations on subsequent episodes revealed that the grid structure used for the July 1995 episode was inappropriate because of unacceptable interactions between the eastern portions of the 12- and 24-km grids in high-speed flows. The RAMS nested grid arrangement used for the other five episodes is shown in Figure 1b. The coarse, intermediate, and fine grids for this grid setup had resolutions of 96-, 24-, and 12-km, respectively.

Before the RAMS meteorological fields can be used, they must be converted from the RAMS nested grid structure to the URM-1ATM multiscale grid structure, which covers the eastern half of the United States (Figure 2). URM-1ATM differs from other air quality models in the way it provides multiscale modeling capability. Whereas other models use grid-nesting techniques, URM-1ATM uses variable size grids to capture the details of pollution dynamics without being computationally intensive. The grid cell dimensions are 192, 96, 48, 24, and 12 km with the finest resolution (12 km) cells following the southern Appalachian Mountains and the adjacent areas.

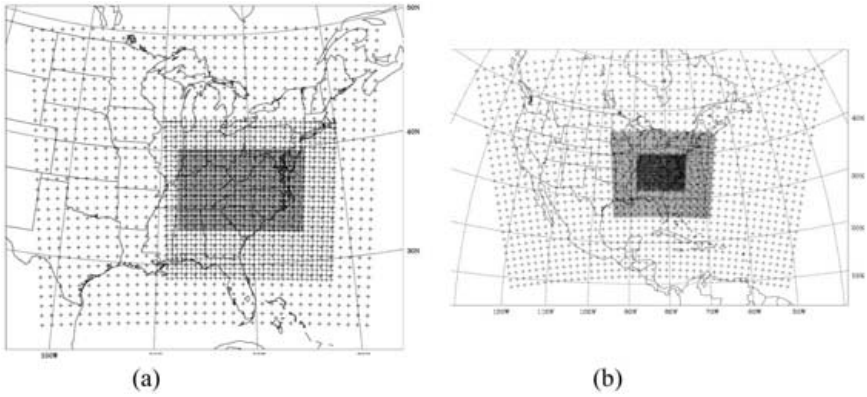

Figure 1. Horizontal grid structures used for the SAMI meteorological modeling. (a) Grids used for the July 1995 episode. (b) Grids used for the other five episodes. Only every other grid point is plotted.

The grid nests in RAMS are arranged such that there is always meteorological data available at the resolution of the URM-1ATM grid. The RAMS and URM-1ATM vertical grids are also different. Though the two grids do match in the vertical extent (i.e., 12,867 m), the RAMS vertical structure has 31 layers, whereas the URM-1ATM vertical structure has 7 layers (Table 1). Hence, it is necessary to aggregate the higher-resolution RAMS layers into the more coarse URM-1ATM layers. A distance-weighting scheme is used to interpolate the scalar fields in the vertical. The use of finer resolution near the surface of the domain, as compared with the more coarse resolution aloft, allows capturing of the steeper concentration gradients in the boundary layer.

Analysis Methods

In contrast to many air quality modeling efforts, SAMI's primary interest is in assessing the impact of emission control scenarios on visibility and the ecosystems (aquatic and terrestrial) in the Southern Appalachian Mountains. Specific focus is placed on air quality in the national parks and wilderness areas designated as Class I.[27] This requires consideration of longer-term air quality metrics, such as the responses of seasonal cumulative ozone, annual average $PM_{2.5}$ (by species), and annual average acid deposition to emission controls. Given the choice of modeling several continuous years (1 year likely will not be representative) or selecting a series of episodes specifically chosen to characterize longer-term meteorology and air quality, SAMI opted for the latter as being more tractable. This modeling approach was designed to provide insight into the atmospheric response to different emission strategies under a variety of conditions. It was also meant to provide a framework for scaling episodic model results to seasonal and annual impacts.

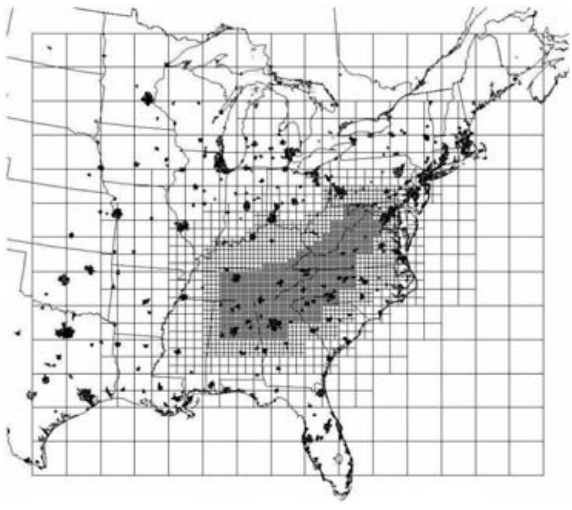

Figure 2. Map of the SAMI modeling domain and multiscale grid structure. The grid sizes range from 12 to 192 km with intermediate values of 24, 48, and 96 km.

Episode Selection and Weighting Scheme

The objective of the episode selection process was to select several multiday episodes to represent the seasonal ozone, annual visibility, and annual acid deposition at Great Smoky Mountains National Park (GRSM) and Shenandoah National Park (SHEN). These two sites were chosen because they had the most complete datasets, are spatially representative of other Class I areas in the SAMI domain, and are the most visited Class I areas in SAMI region. Data classification and optimization techniques[12] were used to select six episodes, each 6–9 days long (plus 2 ramp-up days), between the years 1991 and 1995. These same techniques were later used to select an additional three episodes, but these results will not be presented here, because another research team analyzed the additional episodes.

Table 1. Vertical structure of the URM-1ATM model.

Layer	Coverage (m)[a]	Thickness (m)
1	0–19	19
2	19–62	43
3	62–494	432
4	494–1493	999
5	1493–3272	1779
6	3272–6860	3588
7	6860–12867	6007

[a]Above ground level.

To initiate the episode selection process, each day (or week in the case of acid deposition) is assigned a statistically defined category or class depending on the observed pollutant levels. SAMI categorized individual days into one of four ozone classes. The ozone-classifying variable was the observed daily cumulative ozone exposure using the W126 metric,[27] which is calculated as a weighted sum of hourly ozone concentrations. Ozone W126 was selected, because it can be used to evaluate the ozone effects on forests and vegetation. Only the days during the ozone season (April–October) were considered. Visibility class (1–5) was defined as one of five levels representing the measured daily total fine aerosol mass (sulfate, nitrate, organics, and soils). Wet deposition class (1–4) was defined as one of four levels representing the observed sum of selected cations (calcium and magnesium) and anions (sulfate and nitrate) in weekly precipitation. Dry deposition classes were assigned after the episodes were selected. Wet and dry deposition classes were based on weekly monitoring data, because daily measurements were not available. In each case, class number increased with the severity of pollutant levels with class 1 day being the least polluted and class 4 or 5 days being the most polluted. Ozone classifications 1, 2, 3, and 4 were defined by the cleanest 70% days, next 20% cleanest days, next 7% cleanest days, and the 3% most polluted days, respectively. Then, historic ambient air quality and meteorological data from the 1991–1995 time period was used to classify each day using the Classification and Regression Tree analysis (CART)[28] into specific "bins" that represents similar patterns of meteorology within similar ranges of observed air quality classes.

These CART bins were then used to select a set of multiday episodes to represent a variety of ozone, visibility, and deposition conditions for modeling. The episode selection software attempts to optimize across the pollutants and class I areas in an effort to minimize the errors associated with using a set of episode days to represent annual or seasonal air quality metrics. This is achieved by creating several "scaling factors," which try to account for unrepresented bins, unrepresented classes, and misclassified days. The complete equation[12] to calculate the annual and/or seasonal metrics is:

$$A = \frac{1}{S}\left[\frac{N}{\sum P_k}\right]\sum_{k=1}^{nclass}\left\{\left(\frac{\sum_{j=1}^{b_k} P_j}{\sum_{l_k} P_{l_k}}\right)\left[\sum_{l_k}\left(\frac{WA_{l_k}}{WP_{l_k}}\right)\left(\frac{n_{l_k}}{m_{l_k}}\right)\sum_{j=1}^{m_{l_k}} a_{jl_k}\right]\right\} \quad (1)$$

where A = the value of the metric because of all selected, representative days; S = the number of seasons or years included in the dataset; N = the total number of days included in the dataset; P_j = the number of days in bin j ($P_j = n_j$ whether the user specifies that all days can be used to represent the bin; when only properly classified days are used, they may differ); *nclass* = the number of distinct values of the classification variable; b_k = the number of bins with predicted value k of the classification variable; WA_j = the wt for bin j using all days in bin j; WP_j = the wt for bin j using only properly classified days or all days in bin j, depending on the user's specification; l_k = runs over all bins with the classification value k, from which a representative day was chosen n_j = the number of properly classified days or all days in bin j, depending on the user's specification; m_j = the number of representative days chosen from bin j; and a_{jk} = the observation-based value of the metric for representative day j in bin k.

The *WA/WP* portion of the equation is a scaling factor to account for misclassified days, the P_j/P_l portion is a scaling factor to account for unselected bins within each class, and the N/P_k portion is a scaling factor to account for classes not selected. Because eq 1 is in the form of a weighted contribution multiplied by a bin-based observation, the episode selection software can output all of the information necessary to recalculate the annual and/or seasonal metrics along with the episode weights for selected episode days. In most cases, the error term is <10%.

To calculate a seasonal or annual average metric at each site, the following equation was used:

$$M = \sum_{i=1}^{d}\frac{w_i c_i}{100} \quad (2)$$

where M is the simulated seasonal or annual average pollutant value, d is the number of weighted days (or weeks) contributing to the metric, w_i is the percent contribution of the period i to the metric, and c_i is the simulated daily (or weekly) pollutant value. Note that the averages are composites based on weighting of d events taken between 1991 and 1995. They are surrogates for a seasonal or annual average but are not real in the sense of a true averaging of concentrations simulated throughout an entire season or a year.

Model Performance

Because each episode characterizes a certain fraction of a typical season or year, it is important to evaluate the performance of the model across the range of conditions represented by these episodes. Comprehensive statistical calculations have been performed for each species contributing to the seasonal and annual metrics to determine the ability of the model to accurately estimate ambient

ozone, PM, and acid deposition levels. Among the statistical measures examined are mean normalized bias and mean normalized error. The monitoring networks used for comparison include the National Weather Service for meteorology, Aerometric Information Retrieval System (AIRS) for ozone, Interagency Monitoring of Protected Visual Environments for aerosols, National Atmospheric Deposition Program for wet deposition, and Atmospheric Integrated Research Monitoring Network for dry deposition. Model performance for meteorology, ozone, wet deposition, and dry deposition was computed using observations within the 12-km grid. PM performance was determined from data collected at sites in the 12-, 24-, 48-, and 96-km grids because of the small quantity of data available on the finest grid alone. The remainder of this article discusses the details of the ozone model performance. Part II[29] describes the model performance of the PM components of the model. A comprehensive set of atmospheric modeling results for this project can be found in SAMI's air quality modeling final report[30] and on the Georgia Tech web site.[31]

Meteorological performance statistics were calculated based on all available surface National Weather Service observations within the RAMS 12-km domain (typically on the order of 100 stations) for each episode. The meteorological model performance was compared with other RAMS and MM5 evaluations carried out by Alpine Geophysics and others across the United States over the past 5 years, and the results were considered to be adequate for the SAMI modeling requirements and consistent with the current capabilities of meteorological models in general.[21]

Hourly and 8-hr Average Ozone Model Performance Evaluation Metrics

Statistical calculations were made to evaluate the ability of the modeling system to accurately estimate ambient ozone concentrations for four episodes representing the ozone season. The February 8–13, 1994, and March 23–31, 1993, episodes were not examined. Ozone statistical calculations were done using the Modeling Analysis and Plotting System package.[32] Observations used in these calculations were obtained from the AIRS database.[33] Among the statistical measures that were examined were the mean normalized bias and the mean normalized error. There are several hundred AIRS stations within the modeling domain reporting data during the four ozone episodes. However, some of these stations fall into coarse resolution cells where the model predictions may be subject to large inaccuracies. Therefore, only the stations falling within the 12-km grid are used in the performance analysis.

$$MNB = \frac{1}{N}\sum_{i=1}^{N}\frac{(c_i^e - c_i^o)}{c_i^o} \times 100\% \quad (3)$$

$$MNE = \frac{1}{N}\sum_{i=1}^{N}\frac{|c_i^e - c_i^o|}{c_i^o} \times 100\% \quad (4)$$

where c_i^e is the model-estimated concentration at station i, c_i^o is the observed concentration at station i, and N equals the number of estimate-observation pairs drawn from all valid monitoring station data for the specific day of interest. Because the normalized quantities can become large when the observations are small, a threshold value of 40 ppb is used in conjunction with eq 3 and 4. Whenever the observation is smaller than the threshold value, that estimate-observation pair is excluded from the calculations.

Daily Ozone W126 Model Performance Evaluation Metric

Ozone W126 is used to represent the cumulative seasonal exposure to ozone. The W126 exposure index[27] was selected to characterize ozone trends and relate vegetation yield reduction to ozone exposure. The daily cumulative ozone W126 is calculated using equation 5 and the sigmoid weight function (f_i) given in equation 6:

$$W126 = \sum_{i=1}^{24} c_i f_i \quad (5)$$

$$f_i = \frac{1}{1 + Me^{-Ac_i}} \quad (6)$$

where, c_i is the hourly ozone concentration in ppb, f_i is the weighting factor, M is 4403, and A is 0.126 ppb^{-1}. M and A are arbitrary positive constants that were subjectively determined to develop a weighting function that did the following: (1) focused on hourly average ozone concentrations as low as 40 ppb, (2) had an inflection point near 65 ppb, and (3) had an equal weighting of one for hourly average ozone concentrations at ~100 ppb and above.[27] The W126 index focuses on the higher hourly average concentrations, while retaining the mid- and lower-level values. A seasonal cumulative reconstructed ozone W126 value can be calculated by multiplying the seasonal average reconstructed ozone W126 values from equation 5 by the number of days in the ozone season (214 days).

RESULTS AND DISCUSSION

The six episodes listed in Table 2 were chosen for detailed modeling. A general description of the severity of the

Table 3. Ozone classes and their contribution (weight) to the seasonal cumulative ozone W126 metrics at GRSM and SHEN.

Date	GRSM		SHEN	
(MM/DD/YY)	Class	Weight (%)	Class	Weight (%)
07/23/91	–	–	3	0.23
07/26/91	3	1.46	2	3.12
07/27/91	2	1.16	–	–
07/28/91	1	8.39	2	3.12
07/30/91	–	–	1	16.10
07/31/91	2	1.16	2	3.12
05/11/93	2	0.84	3	0.23
05/12/93	–	–	3	2.70
05/13/93	1	27.96	1	16.10
05/15/93	2	12.32	–	–
05/16/93	2	0.84	–	–
05/17/93	2	0.52	–	–
05/24/95	3	1.70	3	2.70
05/25/95	3	1.29	2	3.12
05/26/95	3	0.37	–	–
05/27/95	2	4.76	–	–
05/28/95	–	–	1	16.10
05/29/95	1	27.96	1	16.10
07/11/95	3	0.52	3	2.70
07/12/95	3	1.70	3	0.90
07/13/95	3	1.70	4	0.70
07/14/95	4	2.02	4	1.99
07/15/95	3	0.37	4	1.14
07/17/95	3	0.92	2	2.39
07/18/95	–	–	2	3.12
07/19/95	4	2.02	2	4.33

Notes: GRSM = Great Smoky Mountains National Park; SHEN = Shenandoah National Park.

ozone, PM, and acid deposition levels is also included for each episode that will be used to calculate the corresponding seasonal and annual air quality metrics. An additional three episodes were simulated elsewhere[30] but will not be presented here. Table 3 lists the ozone classes for modeled days and gives the percentage contribution (weight) to the seasonal ozone metrics at the GRSM and SHEN National Parks. A brief summary of the important weather systems for each episode is presented below.

Table 2. SAMI episodes and the severity of the pollutant levels used to develop seasonal and annual air quality metrics.

Episode	Ozone W126	PM	Acid Deposition
February 8–13, 1994	N/A	Low	Moderate
March 23–31, 1993	N/A	Low	Moderate
May 11–17,1993	Low to moderate	Moderate	Moderate to high
May 24–29, 1995	Moderate	Moderate	Low to moderate
July 23–31, 1991	Low to moderate	High	High
July 11–19, 1995	High	High	Low

February 8–13, 1994

A major incursion of Arctic air occurred during the period of February 9–11 for the eastern half of the United States and was accompanied by a major ice storm from Texas to Ohio. The heaviest precipitation was in a band from northern Mississippi to West Virginia.

March 23–31, 1993

This period was an active one across the Southeast with parts of Tennessee, Alabama, Georgia, North Carolina, and South Carolina having total precipitation >70 mm.

May 11–17, 1993

Several storm and frontal systems affected the eastern United States during this episode with the heaviest precipitation falling across an area from Missouri and Arkansas southeastward across much of the Southeast.

May 24–29, 1995

An active southwest to northeast storm track brought several storm systems to the eastern United States with the strongest during the period of May 27–29. Precipitation fell over a large part of the eastern United States but with the heaviest amounts over an area extending from Missouri and Iowa eastward to the Ohio River valley and then southwestward to the Gulf coast.

July 23–31, 1991

Several frontal systems moved across the Midwest and then stalled over the Southeast. This resulted in an active and very wet pattern for areas along and east of the Appalachians with locally heavy rains and flooding.

July 11–19, 1995

For much of the United States east of the Mississippi River and north of the Gulf coast the weather was dominated by high pressure at the surface and aloft with light winds, little precipitation, and daily maximum temperatures of 30 °C and above. After July 17–18, a frontal passage for much of the same area brought lower temperatures and humidity. For the SAMI region only light and scattered precipitation occurred during the episode.

The coldest and driest (with regard to the 2-m absolute humidity) episode was February 1994, whereas the warmest and most moist was July 1995. The February 1994 and March 1993 cases were dominated by northeasterly winds. All of the other episodes had predominantly southwesterly winds. As expected, the lightest average

wind speeds were for the summer episodes that also had a tendency to have the largest SD of wind direction. The three wettest cases with respect to the mean total precipitation were the March 1993, July 1991, and February 1994 episodes with values of 57 mm, 52 mm, and 46 mm, respectively. The three driest cases with respect to the same statistic were the July 1995, May 1995, and May 1993 episodes with values of 18 mm, 18 mm, and 19 mm, respectively. The two cases with largest SD of 6-hr precipitation amounts were the July 1991 and July 1995 episodes with values of 11.5 mm and 9.2 mm, respectively. The main mode of precipitation in these summer episodes is convection.

Hourly and 8-hr Average Ozone Model Performance Evaluation Results

Time series plots were used to understand how well the model performed at each site and how performance varied by time of day. These plots present both simulated and observed hourly concentrations throughout the simulation period. With the time series plot, one can determine the model's ability to reproduce the peak, the presence or absence of significant bias and errors within the diurnal cycle, and whether the timing of the estimated peak agrees with the observation. Since SAMI's main concern is for ozone in Class I areas, it is also important to discern between performance at urban sites and high-elevation rural sites.

Examples given here (Figures 3 and 4) show the hourly ozone estimates and measurements at an urban site and a high-elevation rural site. These examples are typical of other urban and high-elevation rural locations across the four ozone episodes examined here. Figure 3 shows ozone model performance at Knoxville, TN (a high elevation urban site) for the May 1993 episode. The model underestimates the peaks on many of the days; however, the daytime variations and the timing of the peaks are in good agreement with the observations. On the other hand, modeled nighttime evolution of ozone is considerably different from observations. The modeled ozone may rise during the night while the observations continue dropping to near-zero levels. This is due to ozone mixing

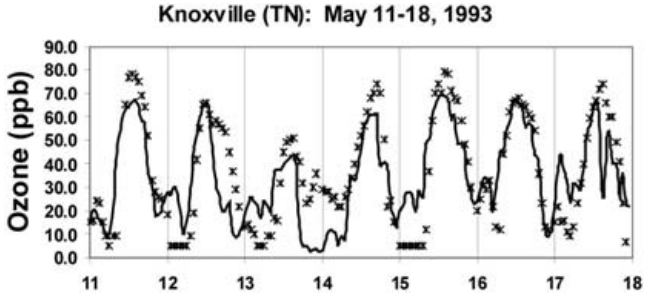

Figure 3. Observed (*) and simulated (-) ozone levels at Knoxville for May 11–18, 1993.

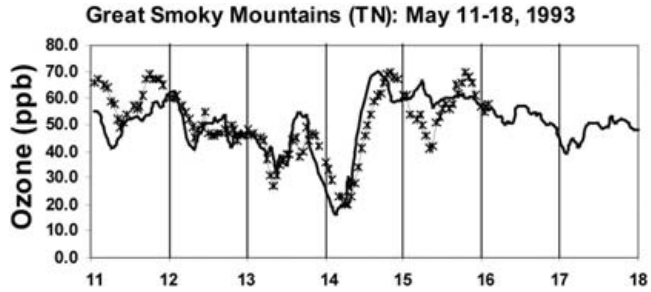

Figure 4. Observed (*) and simulated (-) ozone levels at Great Smoky Mountains for May 11–18, 1993.

from the upper layers of the model along with an underestimation of the nighttime titration of ozone by NO. Figure 4 shows the ozone performance at Great Smoky Mountains (a high-elevation rural sites) for the May 1993 episode (observation were missing for the last 2 days of the episode). High-elevation rural sites typically do not show the diurnal pattern associated with urban sites. The model captures many of the features shown by these observations; however there were some cases where the simulated ozone did not adequately represent observations. Modeled altitudes were much lower than the actual altitudes of these monitoring sites because the 12-km resolution is larger than the mountain peaks; hence the modeled area includes lower elevation regions as well. In such cases, ozone concentrations in the third and fourth layers of the model were often in better agreement with the observations. It is interesting to note that the peak ozone levels at the two sites can be similar, though the average ozone level at the elevated, more remote Class I site is typically higher. This has implications for ozone exposure and damage assessments.

Time series plots are useful for looking at specific stations, but to get an idea of how well the model is performing over all of the stations, the mean normalized bias and error are calculated using the 74 stations falling into 12-km grid cells. Figures 5 and 6 show daily mean normalized biases and errors for hourly (left) and 8-hr averaged (right) ozone concentrations for each day during the four episodes where measurements were available along with EPA's recommended normalized bias and error

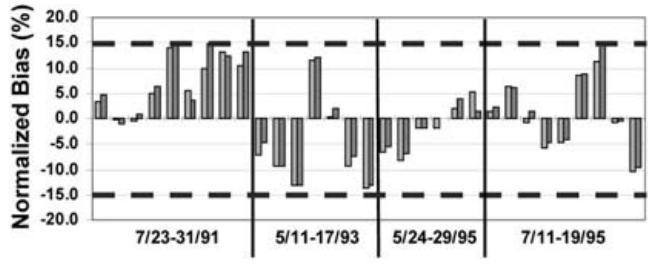

Figure 5. Daily mean normalized biases for hourly (left) and 8-hr average (right) ozone at 74 AIRS sites in the 12-km grid during the four ozone episodes.

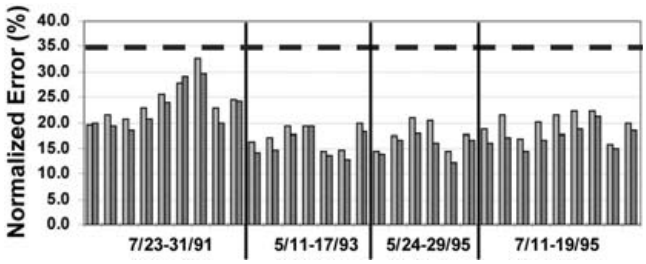

Figure 6. Daily mean normalized error for hourly (left) and 8-hr average (right) ozone at 74 AIRS sites in the 12-km grid during the four ozone episodes.

bounds set for urban-scale modeling.[34] Note that the mean normalized biases are within ±15%, and the mean normalized errors are <35% on all of the modeled days. As expected, the mean normalized bias is similar in direction and magnitude for the hourly and 8-hr averaged calculations. The 8-hr average mean normalized error is typically smaller than the hourly mean normalized error. Mean normalized biases and errors on sequential days of each episode show no evidence of growth in those statistics, and there are no clear signs of a systematic bias.

An analysis of the spatial differences in model performance was performed for hourly ozone on each episode day. Specifically, ozone monitoring sites were divided into 4 groups: (1) high/rural, (2) high/urban, (3) low/rural, and (4) low/urban. The height cut-off to distinguish between high and low elevations was 300 m. Figures 7 and 8 contain the daily mean normalized bias and error for each day during the July 1995 episode. This episode is representative of the spatial differences observed in the other three episodes. Overall, no one grouping is performing better than the others. The bias for the high sites are closer to zero or below zero when the low sites overestimate (July 11, 12, 13, 16, 17), and the bias for the high sites are more negative when the bias at the low sites are negative or close to zero (July 14, 15, 18, 19). From this

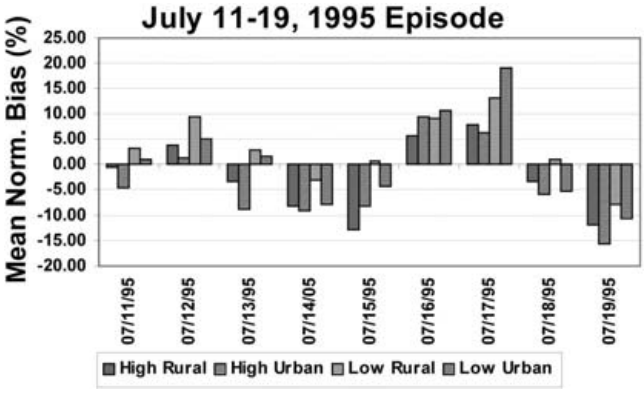

Figure 7. Comparison of daily mean normalized biases for hourly ozone that are segregated by site type (high/low/rural/urban) during the July 11–19, 1995 episode.

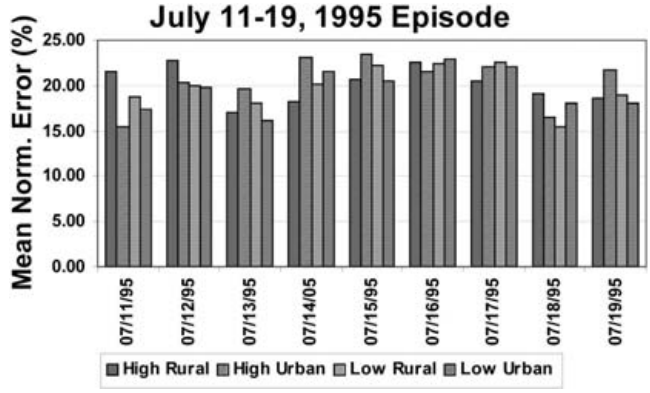

Figure 8. Comparison of daily mean normalized errors for hourly ozone that are segregated by site type (high/low/rural/urban) during the July 11–19, 1995 episode.

analysis, there is no clear trend as to whether urban sites are performing better than rural sites.

Typically, urban applications involve much smaller domains and shorter simulation periods; therefore, urban-scale models can afford finer grid resolution (typically 4 or 5 km) and capture the ozone formation and deposition processes with greater details. Meeting guidelines set for urban-scale models with a regional scale model and for a wide variety of meteorological conditions is encouraging.

Daily Ozone W126 Model Performance Evaluation Results

The ability of the model to simulate ozone W126 was evaluated at 13 stations that represent forested areas in the Southern Appalachian Mountains (Table 4). Because monitoring data is needed for every hour of the day to

Table 4. Monitoring stations where ozone W126 was evaluated.

Monitoring Station	Station ID	Latitude	Longitude	Elevation (m)
Sipsey Wilderness (AL)	SIPS	34.34	−87.34	301
Dawsonville (GA)	DAWS	34.38	−84.06	372
Cranberry (NC)	CRAN	36.01	−81.94	1219
Table Rock (NC)	TBLR	35.80	−81.86	415
Coweeta (NC)	COWT	35.06	−83.43	686
Longcreek (SC)	LONG	34.81	−83.24	658
Great Smoky Mountains NP–Look Rock (TN)	GRSM	35.63	−83.94	793
Speedwell (TN)	SPDW	36.47	−83.83	400
Shenandoah NP–Sawmill Run (VA)	SAWM	38.11	−78.83	445
Shenandoah NP–Big Meadows (VA)	SHEN	38.52	−78.44	1073
Horton Station (VA)	HORT	37.33	−80.55	972
Bearden Knob (WV)	BEAR	39.11	−79.43	1175
Parsons (WV)	PARS	39.09	−79.66	505

calculate the daily ozone W126 concentration, missing data was filled in for each station from 1993–1995 by using monitoring data from a designated neighboring station.[35] SAMI used the TREGRO model[36] to evaluate the benefits to plant species that may occur from ozone concentration decreases because of emission reductions. TREGRO requires a 3-year continuous hourly ozone concentration data set from which daily ozone W126 values were calculated at these 13 stations of interest. Because the years that were used to evaluate the benefits of ozone reductions were 1993–1995, only three of the four ozone episodes were available to evaluate the model performance of daily ozone W126.

Figure 9 contains a comparison ($r^2 = 0.312$) of modeled daily ozone W126 to measured daily ozone W126 at the 13 stations for three episodes (July 11–19, 1995; May 24–29, 1995; and May 24–29, 1993). The model typically overestimates the lower ozone W126 concentrations (<200 ppb) with a mean normalized bias of +242.8%. Modeled ozone W126 values associated with observations >800 ppb were always underpredicted and resulted in a mean normalized bias of −52.9%. For observations in the range of 200–800 ppb, model estimates showed more underpredictions than overpredictions leading to a mean normalized bias of −16%. Recall that the model typically estimates less variability in hourly ozone concentrations than the observations, with the lower concentrations being overpredicted and the daily peaks underpredicted. Because hourly ozone peaks carry the most weight in the daily ozone W126 calculation, it is not surprising that all of the observed ozone W126 values >800 ppb were underestimated by the model.

The mean normalized bias and error were calculated for each model day (all stations) and each station (all days) where ozone W126 values were available. A daily ozone W126 threshold cut-off value of 200 ppb was used in conjunction with eq 3 and 4 to calculate mean normalized bias and error. This threshold value was picked, because it fell between the daily ozone W126 values that would result from using 24 hourly observations of 40 ppb and 60 ppb (EPA's recommended threshold values for hourly ozone). Whenever the observation is smaller than the threshold value, that estimate-observation pair is excluded from the calculations. The overall mean normalized bias and error are −23.4% and 47.2%, respectively. On a day-to-day basis, the model typically underpredicts the daily ozone W126 (18 of 21 days) with the mean normalized bias less than ±50% on 16 of 21 days. The mean normalized error on a day-to-day basis typically ranges from 25% to 75% with a majority of the modeling days falling below 61% (19 of 21 days). To examine the impact of elevation on a station-by-station basis, mean normalized bias (Figure 10) and error (Figure 11) were calculated and grouped by elevation (>600 m versus <600 m). Overall, the mean normalized bias ranges from +22% to −56%, and the mean normalized error ranges from 40% to 60% at each station. There is a clear elevational gradient, with the higher elevation sites typically showing poorer model performance because of large underprediction in ozone concentrations.

It is not surprising that the ozone W126 performance is not as good as the hourly ozone performance presented earlier. One reason for the poorer model performance is that the hourly evaluation included both rural and urban sites, whereas the ozone W126 evaluation was conducted for just 13 rural, high-elevation sites. The complex meteorological conditions associated with elevated, rural sites are usually more difficult to model than conditions at urban sites. Also, photochemical grid models generally have difficulty simulating nighttime mixing. Whereas this in not very important to urban peak ozone concentration, it can be very important for peak ozone concentrations at elevated, rural sites that often occur at night. Because the ozone W126 metric heavily weighs peak

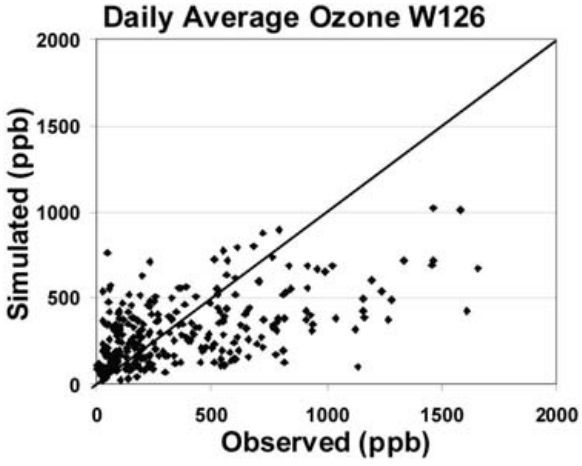

Figure 9. Observed versus simulated daily ozone W126 at 13 monitoring stations representing forested areas in the Southern Appalachian Mountains.

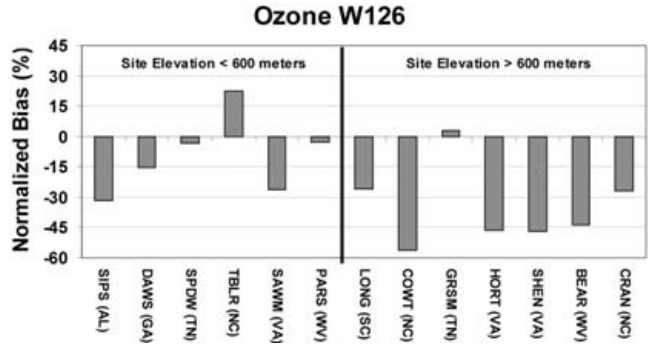

Figure 10. Daily ozone W126 mean normalized bias for 13 monitoring sites representing forested areas in the Southern Appalachian Mountains during the three ozone episodes (see Table 4 for site names and locations).

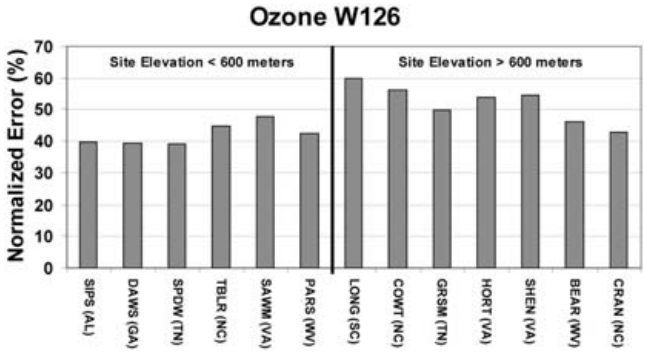

Figure 11. Daily ozone W126 mean normalized error for 13 monitoring sites representing forested areas in the Southern Appalachian Mountains during the three ozone episodes (see Table 4 for site names and locations).

ozone levels, underpredicting peaks can lead to a large negative bias.

Seasonal Average Daily Ozone W126 Model Performance Evaluation

In addition to evaluating the model's ability to simulate ozone W126 values on a day-to-day basis, the resulting seasonal average ozone W126 values at GRSM and SHEN were examined in more detail. This was accomplished by evaluating all of the weighted model days at each site that contributed to the 1993–1995 seasonal average ozone W126 concentration. The daily ozone W126 concentrations on each of these days were multiplied by their percentage of contribution to the seasonal metric and summed to give the seasonal daily average.

Comparisons of observed and modeled ozone W126 at GRSM and SHEN on days that contribute to the seasonal metric typically show an underprediction, especially on the days with the highest observed ozone W126 concentrations. These underpredictions may be because of the inability of the model to account for certain physicochemical processes such as lower stratospheric ozone intrusions at the higher altitude sites. Figures 12 and 13 show the contribution of the individual days to the seasonal daily average ozone W126 concentration at GRSM

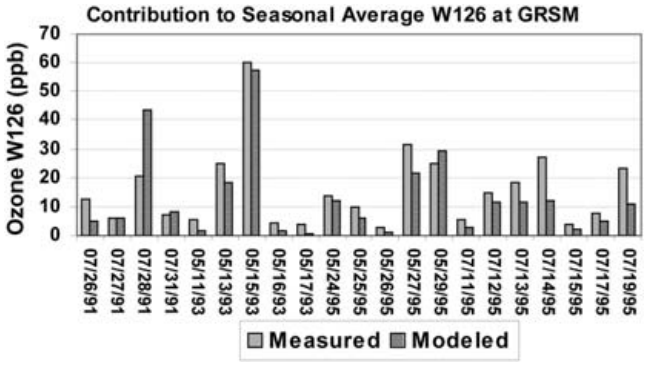

Figure 12. Measured and modeled contributions to the seasonal daily average ozone W126 at GRSM for each weighted episode day.

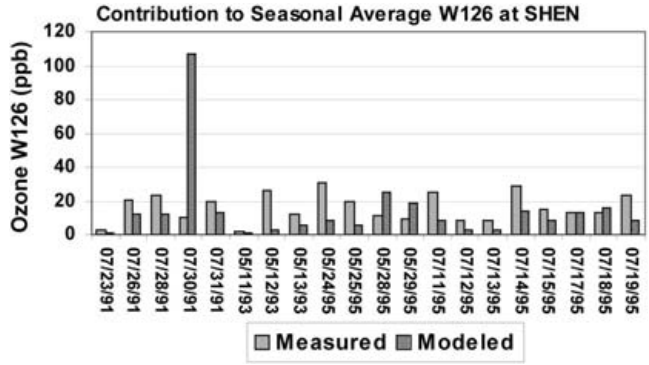

Figure 13. Measured and modeled contributions to the seasonal daily average ozone W126 at SHEN for each weighted episode day.

and SHEN. It is important to get the concentrations correct on the days that contribute most to the seasonal average. At GRSM, the model does a good job of this on four of the seven most important days (>20 ppb contribution) and does an excellent job of representing the most important day (May 15, 1993). Although the modeled and observed ozone W126 concentrations differ on several days, many of these days have smaller contributions to the seasonal average. At SHEN, most of the important days contributing to the seasonal average are underpredicted by ~50%. However, there is one day (July 30, 1991) where the model overpredicts the contribution to the seasonal metric by an order of magnitude.

To evaluate the cumulative effect of each individual day to the seasonal daily average ozone W126, the contributions were summed over all of the weighted days. Figure 14 shows a comparison of the seasonal daily average ozone W126 concentrations at GRSM and SHEN calculated three different ways. The first is the simulated seasonal average ozone W126 value using the modeled daily ozone W126 values multiplied by their specific percentage of contribution for each weighted day at each site. The second bar represents the reconstructed observed ozone W126 value that is calculated using the observed daily ozone W126 values multiplied by their specific percentage of contribution for each weighted day at each site. The third bar is the actual observed seasonal daily average ozone W126 concentration using measurements from the 1993–1995 ozone seasons (April–October). The differences between the reconstructed and actual observed ozone W126 is because of the error inherent to the episode selection process. At both sites, the reconstructed observed seasonal averages are slightly higher than the actual seasonal averages. The model does a good job of simulating the reconstructed seasonal average ozone W126 at both sites. It underpredicts the actual seasonal average ozone W126 at GRSM and SHEN by 16.4% and 7.8%, respectively. Both sites show good agreement with observations, but for different reasons. At GRSM, the

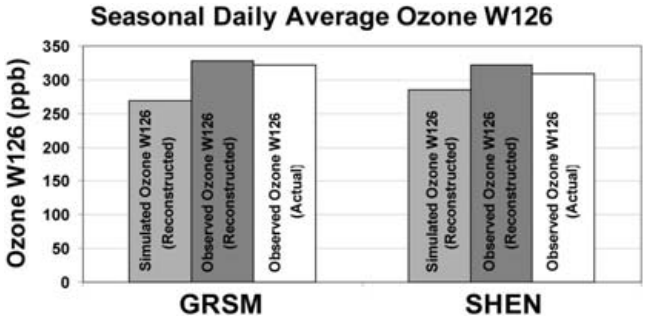

Figure 14. Comparison of modeled and observed seasonal daily average ozone W126 at Great Smoky Mountains (Look Rock) and Shenandoah (Big Meadows) National Parks.

model does a good job of simulating daily ozone W126 on a majority of the most important days (>20 ppb contribution). This is especially true on May 15, 1993, a day that contributes 60 ppb (twice the contribution from the second most important day) to the seasonal average ozone W126 concentration. Because the model does well on the days that contribute the most to the seasonal average, the fact that the model does not do as well on the other days is not as important. However, the reason SHEN shows good agreement with the observed seasonal average is because of compensating errors. Although most modeling days show an underprediction in the daily ozone W126, there is one day (July 30, 1991) that is more than an order of magnitude higher than the observations. This one value is enough to balance the underpredictions on all of the other weighted days leading to a seemingly accurate seasonal average.

Sources of Modeling Uncertainty

There are many known sources of error in running the RAMS/EMS-95/URM-1ATM atmospheric modeling system. First, there are uncertainties associated with the meteorological inputs (e.g., soil moisture) and in the scientific understanding of how to best parameterize/simulate certain meteorological processes (e.g., convection and cloud formation). Some of the more important meteorological parameters, such as temperature, wind speed, and wind direction, can bias the predicted pollutant concentrations and skew the source/receptor relationships. Also, related studies[37] of the SAMI region using similar emission estimates suggest that there are likely significant uncertainties in the emissions; however, no attempts were made here to quantify these uncertainties.

In addition, there are model uncertainties caused by the lack of adequate horizontal and vertical grid resolution, especially in very complex terrain where a coarser grid resolution may not allow the modeling system to capture important subgrid features. Additional modeling limitations likely contributing to discrepancies between the predictions and observations include reduced temporal and spatial variance in emissions compared with actual values, spatial and temporal smoothing of turbulent mixing, extremes in point measurements usually having a greater range than concentrations averaged over the modeling grid, and the inability of the model to reproduce some meteorological and chemical processes occurring at subgrid scales. There are additional errors caused by not modeling large point source plumes at subgrid scale. This can result in plumes being diluted too fast and the chemistry pushed into a different chemical regime. As a consequence, the spatial relationship between pollutant sources and downwind pollutant concentrations can be affected. This list is certainly not exhaustive but addresses some of the major issues SAMI has faced regarding sources of uncertainty in its modeling.

CONCLUSIONS

The RAMS/EMS-95/URM-1ATM atmospheric modeling system was developed to assess how emission controls will affect ozone, PM, and acid deposition in the Southern Appalachian Mountains. This article examined the modeling system's ability to simulate ozone concentrations. In this regional-scale application, simulated hourly ozone concentrations were typically within EPA guidance criteria for urban-scale modeling with mean normalized biases less than ±15% and mean normalized errors <35%. Simulated ozone levels showed less variability than the observations and were generally overestimated when observed levels were low and underestimated when they were high. An analysis of spatial variation in model performance between high/rural, high/urban, low/rural, and high/urban sites did not show any clear trend as to whether urban, rural, high, or low elevation sites were performing better. Also, daily and seasonal ozone W126 concentrations (cumulative exposure index) were modeled and compared with observations. All of these sites examined were high-elevation rural sites and did exhibit a trend of poorer performance for higher elevation sites. Although the performance statistics for daily ozone W126 concentrations were not as good as for the hourly concentrations, the seasonal ozone W126 daily average concentrations matched well with observations. Results here suggest that the atmospheric modeling component of SAMI's integrated assessment will likely introduce a non-negligible, but not dominating, uncertainty.

ACKNOWLEDGMENTS

This research was sponsored by the Southern Appalachian Mountain Initiative (SAMI) under grants from the EPA and the member states. The authors thank the members of the SAMI atmospheric modeling subcommittee and

Southern Company, Duke Power, and TVA for providing day-specific emissions.

REFERENCES

1. Sisler, J.F.; Malm, W.C. Interpretation of Trends of $PM_{2.5}$ and Reconstructed Visibility From the IMPROVE Network; *J. Air & Waste Manage. Assoc.* **2000**, *50,* 775-789.
2. Heck, W.W.; Furiness, C.S.; Cowling, E.B.; Sims, C.K. Effects of Ozone on Crop, Forest, and Natural Ecosystems: Assessment of Research Needs; *EM.* **1998**, *October,* 11–22.
3. Cowling, E.B. Recent Changes in Chemical Climate and Related Effects on Forests in North America and Europe; *AMBIO.* **1998**, *18,* 167-171.
4. Boylan, J.W.; Odman, M.T.; Wilkinson, J.G.; Russell, A.G.; Doty, K.G.; Norris, W.B.; McNider, R.T. Development of a Comprehensive, Multiscale "One Atmosphere" Modeling System: Application to the Southern Appalachian Mountains; *Atmos. Environ.* **2002**, *36,* 3721-3734.
5. Pielke, R.A.; Cotton, W.R.; Walko, R.L.; Tremback, C.J.; Lyons, W.A.; Grasso, L.D.; Nicholls, M.E.; Moran, M.D.; Wesley, D.A.; Lee, T.J.; Copeland, J.H.A. Comprehensive Meteorological Modeling System-RAMS; *Meteor. Atmos. Phys.* **1992**, *49,* 69-91.
6. Wilkinson, J.G.; Loomis, C.F.; McNally, D.E.; Emigh, R.A.; Tesche, T.W; *Technical Formulation Document: SARMAP/LMOS Emissions Modeling System (EMS-95*); AG-90/TS26 & AG-90/TS27. Alpine Geophysics: Pittsburgh, PA, 1994.
7. Odman, M.T.; Russell, A.G. A Multiscale Finite Element Pollutant Transport Scheme for Urban and Regional Modeling; *Atmos. Environ.* **1991**, *25A,* 2385–2394.
8. Kumar, N.; Odman, M.T.; Russell, A.G. Multiscale air Quality Modeling: Application to Southern California; *J. Geophys. Res.* **1994**, *99,* 5385-5397.
9. Kumar, N.; Russell, A.G. Multiscale Air Quality Modeling of the Northeastern United States; *Atmos. Environ.* **1996**, *30,* 1099-1116.
10. Kasibhatla, P.; Chameides, W.L. Seasonal Modeling of Regional Ozone Pollution in the Eastern United States; *Geophys. Res. Lett.* **2000**, *27,* 1415-1418.
11. Bouchet, V.S.; Laprise, R.; Torlaschi, E.; McConnell, J.C.; Plummer, D.A. Studying Ozone Climatology With a Regional Climate Model 2. Climatology; *J. Geophys. Res.* **1999**, *104,* 30373-30385.
12. Deuel, H.P.; Douglas, S.G; *Episode Selection for the Integrated Analysis of Ozone, Visibility and Acid Deposition for the Southern Appalachian Mountains*; SYSAPP-98/07r1. Systems Applications International: San Rafael, CA., 1998.
13. Carter, W.P.L. A Detailed Mechanism for the Gas-Phase Atmospheric Reaction of Organic Compounds; *Atmos. Environ.* **1990**, *24,* 481-518.
14. Carter, W.P.L. Computer Modeling of Environmental Chamber Measurements of Maximum Incremental Reactivities of Volatile Organic Compounds; *Atmos. Environ.* **1995**, *29,* 2513-2527.
15. Nenes, A.; Pilinis, C.; Pandis, S.N. ISORROPIA. A New Thermodynamic Equilibrium Model for Multiphase Multicomponent Inorganic Aerosols; *Aquatic Geochem.* **1998**, *4,* 123-152.
16. Pandis, S.N.; Harley, R.A.; Cass, G.R.; Seinfeld, J.H. Secondary Organic Aerosol Formation and Transport; *Atmos. Environ.* **1992**, *26A,* 2269-2282.
17. Kim, Y.P.; Seinfeld, J.H. Simulation of Multicomponent Aerosol Condensation by the Moving Sectional Method; *J. Colloid Interface Sci.* **1989**, *135,* 185-199.
18. Berkowitz, C.E.; Easter, R.C.; Scott, B.C. Theory and Results From a Quasi-Steady-State Precipitation-Scavenging Model; *Atmos. Environ.* **1989**, *23,* 1555-1571.
19. Wesely, M.L. Parameterization of Surface Resistances to Gaseous dry Deposition in Regional-Scale Numerical Models; *Atmos. Environ.* **1989**, *23,* 1293-1304.
20. Kalnay, E.; Kanamitsu, M.; Kistler, R.; Collins, W.; Deaven, D.; Gandin, L.; Iredell, M.; Saha, S.; White, G.; Woollen, J.; Zhu, Y.; Chelliah, M.; Ebisuzaki, W.; Higgins, W.; Janowlak, J.; Mo, K.C.; Ropelewski, C.; Wang, J.; Leetmaa, A.; Reynolds, R.; Jenne, R.; Joseph, D. The NCEP/NCAR 40-Year Reanalysis Project; *Bull. Amer. Meteor. Soc.* **1996**, *77,* 437-471.
21. Doty, K.G.; Tesche, T.W.; McNally, D.E.; Timin, B.; Mueller, S.F; *Meteorological Modeling for the Southern Appalachian Mountains Initiative (SAMI*). Final Report submitted to Southern Appalachian Mountains Initiative: Asheville, NC, 2001.
22. Pechan/Avanti Group; *Southern Appalachian Mountains Initiative (SAMI) Emissions Projections to 2010 and 2040: Growth and Control Data and Emission Estimation Methodologies*. 01.07.002/9405.000; Draft Final Report submitted to Southern Appalachian Mountains Initiative: Asheville, NC, 2001.
23. U.S. Environmental Protection Agency. *User's Guide To MOBILE5 (Mobile Source Emission Factor Model*). EPA-AA-TEB-94–01; Office of Air and Radiation, Office of Mobile Sources, Emissions Planning and Strategies Division, Air Quality Analysis Branch: Ann Arbor, MI, 1994.
24. Pierce, T.E.; Geron, C.D. *The Personal Computer Version of the Biogenic Emissions Inventory System (PCBEIS2.2)*. AAREADME, anonymous ftp at monsoon.rtpnc.epa.gov located in /pub/beis2/pcbeis22.
25. Pierce, T.E.; Lamb, B.K.; Van Meter, A.R. Development of a Biogenic Emissions Inventory System for Regional Scale Air Pollution Models. In *Proceedings of the 83rd Annual Meeting & Exhibition of A&WMA*, Pittsburgh, PA, 1990.
26. U.S. Environmental Protection Agency. *List of 156 Mandatory Class I Federal Area*. March 2002; available at http://www.epa.gov/oar/vis/class1.html (accessed May 9, 2005).
27. Lefohn, A.S.; Runeckles, V.C. Establishing a Standard to Protect Vegetation - Ozone Exposure/Dose Considerations; *Atmos. Environ.* **1987**, *21,* 561-568.
28. Brieman, L.; Friedman, J.H.; Olshen, R.A.; Stone, C. J. *Classification and Regression Trees*. Belmont, CA: Wadsworth, 1984.
29. Boylan, J.W.; Odman, M.T.; Wilkinson, J.G.; Russell, A.G. Integrated Assessment Modeling of Atmospheric Pollutants in the Southern Appalachian Mountains: Part II-$PM_{2.5}$ and Visibility; *J. Air & Waste Manage. Assoc.* **2004**, submitted for publication.
30. Odman, M.T.; Boylan, J.W.; Wilkinson, J.G.; Russell, A.G.; Mueller, S.F.; Imhoff, R.E.; Doty, K.G.; Norris, W.B.; McNider, R.T. *SAMI Air Quality Modeling Final Report*; Southern Appalachian Mountains Initiative: Asheville, NC, 2002.
31. Georgia Institute of Technology. *SAMI Atmospheric Modeling Home Page*; available at http://environmental.gatech.edu/SAMI (accessed May 9, 2005).
32. McNally, D.E.; Tesche, T.W. *Modeling Analysis and Plotting System User Manual*. Alpine Geophysics: Pittsburgh, PA, 1991.
33. U.S. Environmental Protection Agency; *EPA AIRS Data*. Office of Air Quality Planning & Standards, Information Transfer & Program Integration Division, Information Transfer Group; available at http://www.epa.gov/air/data/index.html (accessed May 9, 2005).
34. U.S. Environmental Protection Agency. *Guidance for Regulatory Application of the Urban Airshed Model (UAM*). Office of Air Quality Planning and Standards: Research Triangle Park, NC, 1991.
35. Weinstein, D.A.; Woodbury, P.B.; Gollands, B.; King, P.; Lepack, L.; Pendleton, D. *Assessment of Effects of Ozone on Forest Resources in the Southern Appalachian Mountains*. Report submitted to Southern Appalachian Mountains Initiative: Asheville, NC, 2002.
36. Weinstein, D.A.; Beloin, R.M.; Yannai, R.D. Modeling Changes in red Spruce Carbon Balance and Allocation in Response to Interacting Ozone and Nutrient Stresses; *Tree Physiol.* **1991**, *9,* 127-146.
37. Mendoza-Dominguez, A.; Russell, A.G. Estimation of Emission Adjustments From the Application of Four-Dimensional Data Assimilation to Photochemical air Quality Modeling; *Atmos. Environ.* **2001**, *35,* 2879-2894.

About the Authors

James Boylan is a senior environmental engineer with the Air Protection Branch of the Georgia Department of Natural Resources and is a research associate at Georgia Institute of Technology. Mehmet T. Odman is a principal research engineer in the School of Civil & Environmental Engineering at Georgia Institute of Technology. James Wilkinson is a senior research engineer at Alpine Geophysics, LLC. Armistead G. Russell is the Georgia Power Professor of Environmental Engineering in the School of Civil and Environmental Engineering at Georgia Institute of Technology, Atlanta, GA. Kevin Doty is a research scientist and William Norris is a senior research scientist in the Earth Science Laboratory at the University of Alabama in Huntsville. Richard McNider is a professor in the Department of Mathematical Sciences at the University of Alabama in Huntsville. Address correspondence to: James Boylan, 4244 International Parkway, Suite 120, Atlanta, GA 30354; phone: +1-404-362-4851; fax: +1-404-363-7100; e-mail: james_boylan@dnr.state.ga.us.